Journal of
Mechanical
Science and
Technology

Journal of Mechanical Science and Technology 21 (2007) 755~763

Robust Control of Hydraulically Operated Gimbal System

Taik-Dong Cho[b], Sang-Min Yang[a,*]

[a]*School of Department of Mechanical Design Engineering, Chungnam National University 220 Gung-Dong Yuseong-gu Daejeon 305-764, Korea*
[b]*BK21 Mechatronics Group, Chungnam National University 220 Gung-Dong Yuseong-gu Daejeon 305-764, Korea*

(Manuscript Received June 21, 2006; Revised February 13, 2007; Accepted March 4, 2007)

Abstract

A transmitting antenna operated on the naval vessels can be easily excited by exogenous disturbances such as tidal wave and impact. Gimbal system that supports the antenna needs the controller to maintain the robust performance against various modeling uncertainties and disturbance. PI controller, however, cannot guarantee the reasonable robust performance under these kinds of severe conditions. Thus a robust H_∞ control scheme is recommended to ensure a specified dynamic response under heavy operating conditions. Gimbal system is simplified as two degree of freedom model that ignores coordinate co-relations of each direction and hydraulic system is modelled linearly. The simulation and experimental results of H_∞ controller proposed in this paper showed the better responses and stability than those of PI controller.

Keywords: Single rod hydraulic cylinder; H_∞ control; Robust control; Gimbal system; Hydraulic system

1. Introduction

A high-frequency jamming signal transmitting antenna (hereafter will be referred to as a transmitting device) on a naval vessels is a device to transmit electromagnetic waves to a target. This is very sensitive to vibration and impact because it consists of many optical devices and expensive electronic elements. Additionally, it is not easy to transmit electromagnetic waves precisely to a target because of vessel's rolling, pitching, and yawing motion. Therefore, it is necessary to set up a gimbal system, which keeps the transmitting device horizontal without being affected by the complicate motion of the vessel. The gimbal system on the vessel, however, uses a single-rod hydraulic piston that has model uncertainties. Moreover, because of disturbances (waves and strong wind etc.), the stability of the transmitting device cannot be guaranteed by single input and single output controlling methods, such as the traditional PID controller. Therefore the robust control algorithm is desired to get a better control of the gimbal system.

As mentioned, it is not easy to guarantee the stability and acceptable performance by the PID controller, because the system has much unexpected disturbances and model uncertainties. The LQ controller has to observe every state to make the suitable controller. This means that there are many limitations especially when it is not easy to measure every state variable. The LQG/LTR is another optimized H_2 control theory which minimizes the cost function in the form of the square. This method guarantees the stability and good performance, but it still has a disadvantage that it does not take into consideration the uncertainty of the system or the stability margin for the disturbances.

*Corresponding author. Tel.: +82 42 821 7625; Fax.: +82 42 821 7625
E-mail address: s_smyang@cnu.ac.kr

There has been many researches on the robust control to improve the control performance of a system that has model uncertainties and disturbances. Zames(1981) suggested minimizing the excessive sensitivity function in the every frequency range for the problem of H_∞ in the single input single output(SISO) system. Glover and Doyle(1989) announced a solu-tion in which the given close loop transfer function was smaller than the given value γ of H_∞-norm, and this solution could also stabilize the plant in every state space. This method showed the collection of all controllers which satisfied a condition by $Q(s)$ by using two Riccati algebra equations. Park et. al(2005) de-monstrated the feasibility of active control of beams with a mix of beams with a mix of H_∞ and H_2 and performance. In this study, a robust controller (H_∞ controller) has been designed and applied for the horizontal control of a hydraulic-operated gimbal system that has disturbances and uncertainty of the system.

2. The modeling of the gimbal system

2.1 The kinematic behavior of the gimbal system

The experimental system consists of the bottom (body 1) and the upper plates(body 2). The bottom plate corresponds to the deck of the vessel, and the upper plate is controlled to be maintained in horizontal state. These two plates are connected with a hydraulic cylinder making relative motion possible.

Figure 1 shows the schematic diagram of the gimbal system. It is designed to control the angular move-ment of the body 2 against the motion of body 1, which corresponds the vessel. Figure 2 displays a sim-plified diagram for mathematical modeling of Fig. 1.

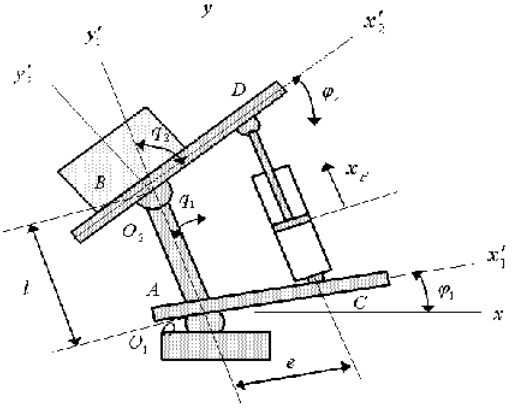

Fig. 1. Schematic diagram of the gimbal system.

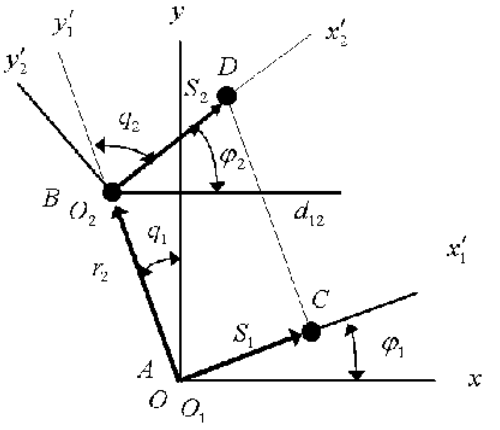

Fig. 2. Schematic diagram for modeling.

axy is the fixed coordinate. $a_1x_1'y_1'$ is the moving coordinate of body 1 and $a_1x_2'y_2'$ is the moving coordinate of body 2. The centroids of each object O_1 are O_1 and respectively. With generalized coordinate for the rotating degree of body 1 and for the relative rotating degree of body 2 against body 1, the displacement and acceleration of body 2 are as in Eqs. (1) and (2).

$$r_2 = \begin{bmatrix} x_2 \\ y_2 \end{bmatrix} = \begin{bmatrix} -l\sin q_1 \\ l\cos q_1 \end{bmatrix} \tag{1}$$

$$\dot{r_2} = \begin{bmatrix} -l\cos q_1 \\ -l\sin q_1 \end{bmatrix} \dot{q_1} = \begin{bmatrix} l\sin q_1 \\ -l\cos q_1 \end{bmatrix} \dot{q_1}^2 \tag{2}$$

If all the friction forces on the system are neglected, the virtual work with hydraulic cylinder force F_u is given as the following Eq.(3).

$$\begin{aligned} \delta W &= -Fu\delta L \\ &= [\delta r_2^T \delta\varphi_2]\frac{F_u}{L}\begin{bmatrix} d_{12} \\ d_{12}^T B_2 S_2 \end{bmatrix} \\ &+ [\delta r_1^T \delta\varphi_1]\frac{F_u}{L}\begin{bmatrix} d_{12} \\ d_{12}^T B_1 S_1 \end{bmatrix} \end{aligned} \tag{3}$$

where, S_1 and S_2 are vector O_1C and O_2D, and d_{12} is the distance vector and Length(L) is $L^2 = d_{12}^T d_{12}$ between both ends of the cylinder and . is rotation transformation matrix. and can be expressed as in Eqs. (4) and (5).

$$d_{12} = \begin{bmatrix} x_2 \\ y_2 \end{bmatrix} + e\begin{bmatrix} \cos\varphi_2 \\ \sin\varphi_2 \end{bmatrix} - e\begin{bmatrix} \cos\varphi_1 \\ \sin\varphi_2 \end{bmatrix} \tag{4}$$

$$Bi = \frac{d}{d\varphi_1}\begin{bmatrix} \cos\varphi_i & -\sin\varphi_i \\ \sin\varphi_i & \cos\varphi_i \end{bmatrix},\ i = 1, 2 \tag{5}$$

Therefore, the generalized force can be obtained as

$$\begin{bmatrix} F_1 \\ T_1 \end{bmatrix} = \begin{bmatrix} (F_u / L)d_{12} \\ (F_u / L)d_{12}^T B_2 S_1 \end{bmatrix} \tag{6-a}$$

$$\begin{bmatrix} F_2 \\ T_2 \end{bmatrix} = \begin{bmatrix} (-F_u / L)d_{12} \\ (-F_u / L)d_{12}^T B_2 S_2 \end{bmatrix} \tag{6-b}$$

The equation of the motion of the system consisting of body 1 and 2 and being moved by the hydraulic cylinder force, is

$$\sum_{i=0}^{2}[\delta r_i^T (m_i \ddot{r}_i - F_i) + \delta\varphi_i (J_i\ddot{\varphi}_i - T_i)] = 0 \tag{7}$$

Since Eq.(7) is applied only to body 2 corresponding the transmitting device ignoring the movement of body 1, Eq.(7) can be expressed as

$$\left[\delta r_2^T (m_2\ddot{r}_2 - F_2) + \delta\varphi_2 (J_2\ddot{\varphi}_2 - T_2)\right] = 0 \tag{8}$$

Eq.(9) can be derived from Eq.(8) and, the motion of body 2 can be obtained from Eq.(9) as shown in Eq.(10).

$$\begin{bmatrix} 2J_2 + m_2 l^2 - J_2 \\ -2J_2 \qquad J_2 \end{bmatrix}\begin{bmatrix} \ddot{\varphi}_1 \\ \ddot{\varphi}_2 \end{bmatrix} + \begin{bmatrix} (F_u e / L)[l + e\sin(\varphi_2 - \varphi_1)] \\ -(F_u e / L)[l\cos(\varphi_2 - \varphi_1) + e\cos(\varphi_2 - \varphi_1)] \end{bmatrix} = 0 \tag{9}$$

$$J_2\ddot{\varphi}_2 = \frac{F_u e}{L}[l\cos(\varphi_2 - \varphi_1) + e\sin(\varphi_2 - \varphi_1)] + 2J_2\ddot{\varphi}_1 \tag{10}$$

If and are not large and the angular acceleration of vessel is small, Eq.(11) can be obtained by applying $l_p = l$ and $\ddot{\varphi}_1 = 0$.

$$J_2\ddot{\varphi}_2 = F_u e \tag{11}$$

Eq.(11) means that body 2, a gimbal system, does not depend on the movement of body 1, but it is a simple 2-degree-of-freedom device, which rotates independently in each fixed coordinate. If we assume the rotating angles of vessel deck and the gimbal system are very small, Eq.(12) is obtained because $e\phi = x_p$ and $e\varphi_1 = x_d$.

$$x_p = e\varphi_2 - x_d \tag{12}$$

where x_p the displacement of piston, e the distance from the central axis to the piston, and ϕ the horizontal angle of the gimbal system.

2.2 The modeling of single-rod hydraulic system

The dynamic characteristics of servo valves is generally expressed as the 1st order system dimension function in the low-frequency region. The relationship between operating current $I(s)$ and spool displacement $X_v(s)$ of servo valves is expressed as in Eq.(13).

$$\frac{X_v(s)}{I(s)} = \frac{K_{sv}}{\tau_v s + 1} \tag{13}$$

where $X_v(s)$ the spool displacement of servo valves, K_{sv} gain, and τ_v time constant.

Figure 3 shows a single-rod hydraulic cylinder. Because the hydraulic areas of the piston are different, the dynamic characteristics of the cylinder includes nonlinearity and the travel speeds in both direction are different. The nonlinearity of a single-rod hydraulic cylinder is conveniently modeled mathematically as an additional disturbance. And then, we model it with the same linear analysis as that of double-rod cylinder. The flow rate equation of the

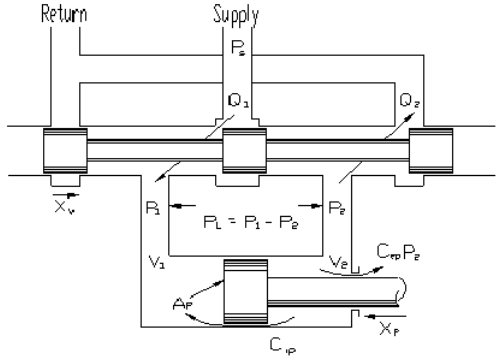

Fig .3. Single-rod hydraulic cylinder.

servo valve with a single-rod hydraulic cylinder can be determined defined as in Eqs. (14) and (15) from the equations derived the direction of $\dot{x}_p$.

$$Q_L = \frac{Q_1 + Q_2}{2} \tag{14}$$

$$Q_L = \alpha C_d w x_v \sqrt{\frac{1}{\rho}\left(P_s - \frac{x_v}{|x_v|} P_L \right)} \tag{15}$$

where, $\alpha = \dfrac{1+n}{\sqrt{2(1+n^2)}} \le 1$.

Eq.(15) is the flow rate equation of the servo valve with a single-rod hydraulic cylinder. It can be linearized by Taylor expansion series near the operating point (x_v, P_L^*) as in Eq.(16).

$$Q_L = K_q x_v - K_c P_L \tag{16}$$

where,

$$K_q = \frac{\partial Q_L}{\partial x_v} = \alpha C_d w \sqrt{\frac{1}{\rho}(P_x + P_L^*)} \tag{17}$$

$$K_q = \frac{\partial Q_L}{\partial P_L} = \frac{\alpha C_d w x_v^*}{2\sqrt{\rho(P_s - P_L)}} = \alpha C_d w \sqrt{\frac{1}{\rho}(P_x + P_L^*)} \tag{18}$$

Eq.(19) is the flow rate equation of the servo valve with a single-rod hydraulic cylinder.

$$Q_L = A_{me}\dot{x}_p + C_{tp} P_L + \frac{V_e}{4B_e}\dot{P}_L \tag{19}$$

where the average piston area, and C_{tp} total leakage coefficient of the piston. A_{me} and V_e the equivalent volume of the hydraulic cylinder are expressed as Eqs. (20) and (21).

$$A_{me} = \frac{(1+\eta)a}{2(1-\eta)} \tag{20}$$

$$V_e = A_e L_s \tag{21}$$

where η flow ratio, L_s cylinder travel and a the cross section area of the piston rod with $A_e = (1+\eta^3)a / (1+\eta^2)(1-\eta)$.

Eq.(22) can be obtained from Eq.(11), which is the equation of motion of the gimbal system, with $F_u = L_s A_e P_L$.

$$\theta(s) = \frac{K_q x_v(s) + A_{me} x_d(s) s}{s\left(\dfrac{V_e}{4\beta_e}\dfrac{J_o}{eA_e}s^2 + K_{ce}\dfrac{J_o}{eA_e}s + A_{me}e\right)} \tag{22}$$

where $K_{ce} = K_c + C_{tp}$.

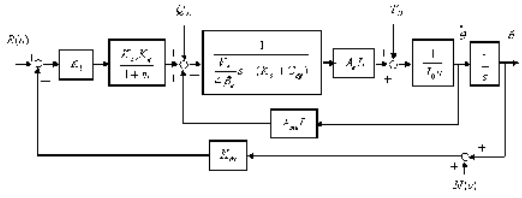

Fig. 4. Block diagram of the electro-hydraulic system.

If K_c is linearized around the valve zero position, the transfer function of the servo valve, piston, and load can be expressed as in Eq.(23) by linear analysis of hydraulic system since K_c=0.

$$\theta(s) = \frac{K_{sv} K_q(s) + A_{me} x_d s(1+\tau_v s)}{s(1+\tau_v s)\left(\dfrac{V_e}{4\beta_e}\dfrac{J_o}{eA_e}s^2 + K_{ce}\dfrac{J_o}{eA_e}s + A_{me}e\right)} \tag{23}$$

Figure 4 shows the block diagram of the single-rod hydraulic gimbal system. If we define x and v as $x = \left|\theta\dot{\theta}P_L\right|$ and $v = \left|Q_D T_D\right|$, the state-space model of hydraulic system can be obtained. The time constant τ of the servo valve is very small, compared to the dynamic behavior of hydraulic system. So it can be ignored.

3. Design of the H_∞ controller

As time goes on the characteristics of a system or the surrounding conditions (load or disturbances) can be changed in actual condition. Therefore, the control system should be able to adjust by itself to these variations. In addition, some factors are ignored to make model simple in the course of system modeling(Park ,1996).

Because these factors with nonlinearity make the system develop unpredictable behaviors, they can cause serious problems about the stability. H_∞ controller minimizes H_∞-norm of the output from input distur-bances. It is designed as a system which has 2 inputs and outputs as in Fig. 5. In Figure 5, u is the control input, w is external disturbances, y is the

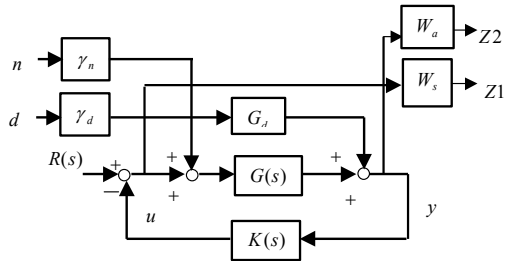

Fig. 5. The closed loop system for loop shaping problem.

output signal of the system, and z is control output signal.

A system as in Fig. 5 needs to be designed as an efficient controller robust to the low-frequency disturbances and the high-frequency noise. A robust controller is designed to keep the robustness from modeling errors and external inputs and to improve the tracking performance of the commands.

The transfer function with respect to the system and the disturbances can be expressed as in Eq.(24).

$$G = \begin{bmatrix} A_g & B_g \\ C_g & D_g \end{bmatrix}, \quad G_d = \begin{bmatrix} A_g & E_g \\ C_g & 0 \end{bmatrix} \tag{24}$$

The expanded transfer function P considering disturbances is given as following Eq.(25).

$$P(s) = \begin{bmatrix} P_{11} & P_{12} \\ P_{21} & P_{22} \end{bmatrix} \tag{25}$$

where,

$$P_{11} = \begin{bmatrix} W_1 & -W_1W_n & -W_1G_dW_d \\ 0 & 0 & 0 \\ 0 & 0 & W_3G_dW_d \end{bmatrix}, \quad P_{12} = \begin{bmatrix} -W_1G \\ W_2 \\ W_3G \end{bmatrix},$$

$$P_{21} = \begin{bmatrix} 1 \\ -W_n \\ -G_dW_d \end{bmatrix}, \quad P_{22} = [-G]$$

W_1, W_2, W_3, W_n and W_d are the weight function to improve the system performance(Lu, 1993; Postlethwaite, 1991). $F_l(P, K_\infty)$ can be obtained from the expanded transfer function, as in Eq.(26). The control problem of is as in Eq.(27).

$$\begin{aligned} Z &= [P_{11} + P_{12}K_\infty(I - P_{22}K_\infty)^{-1}P_{21}]w \\ &= F_l(P, K_\infty) \end{aligned} \tag{26}$$

$$\begin{aligned} &\left\| F_l(P, K_\infty) \right\|_\infty \le \gamma \\ &\left\| \begin{matrix} W_1SG_dW_d \\ W_2RW_n \end{matrix} \right\|_\infty \le \gamma \end{aligned} \tag{27}$$

where, $S = \dfrac{1}{1 + GK_\infty}$, $R = \dfrac{K_\infty}{1 + GK_\infty}$.

Eq.(27) shows that by changing weight value properly, the transfer function of the system can be adjusted as wanted. From Eq.(27), we can see the relationship between weight function and transfer function of the system. S (sensitivity function) and R (complementary sensitivity function) determine the characteristics of the system(Franchek, 1996; McFarlane, 1992). S represents robustness of the system with respect to the disturbances, in other words, the performance of disturbance removal, while R represents the tracking performance of commands. Therefore, we can determine the transfer function of the system by adjusting the weight function appropriately and then improve its performance. The systems applied to this research may be expressed as in the following state Eq.(28).

$$\begin{aligned} \dot{x} &= Ax + B_1w + B_2u \\ z &= C_1x + D_{11}w + D^{12}u \\ y &= C_2x + D_{21}w + D_{22}u \end{aligned} \tag{28}$$

where,

$$A = \begin{bmatrix} A_g & 0 & 0 \\ -B_{w1}C_g & A_{w1} & 0 \\ 0 & 0 & A_{w2} \end{bmatrix},$$

$$B = \begin{bmatrix} 0 & 0 & \gamma_dE_g \\ Bw1 & -\gamma_nB_{w1} & 0 \\ 0 & 0 & 0 \end{bmatrix}, B_2 = \begin{bmatrix} B_g \\ 0 \\ B_{w2} \end{bmatrix}$$

$$C_1 = \begin{bmatrix} 0 & C_{w1} & 0 \\ 0 & 0 & C_{w2} \end{bmatrix}, C_2 = \begin{bmatrix} -C_g & 0 & 0 \end{bmatrix}$$

$$D_{11} = \begin{bmatrix} 0 & 0 & 0 & 0 \\ 0 & 0 & 0 & 0 \end{bmatrix}, D_{12} = \begin{bmatrix} 0 \\ D_{w2} \end{bmatrix},$$

$$D_{21} = [I], D_{22} = [0]$$

$$w = \begin{bmatrix} Q_D \\ T_D \\ n \end{bmatrix}, z = \begin{bmatrix} z_1 \\ z_2 \end{bmatrix}$$

Q_D, T_D and n are disturbances, load torque, and

sensor noise, respectively.

By adjusting the weight function properly for the robustness of the system to the disturbances and better command-tracking performance, the transfer function of the system can be determined, and the performance of the system can be improved. For this, we make Eq.(29) designed as follows.

$$W_s = \frac{0.9}{s+9}, W_a = \frac{0.001s}{s+1}, \quad \gamma_d = 350, \gamma_n = 0.002 \tag{29}$$

$$K(z) = \frac{30.6z^4 - 11.03z^3 - 29.3z^2 - 0.36z + 11.23}{z^5 - 0.84z^4 - 0.8z^3 + 0.48z^2 + 0.36z - 0.18} \tag{30}$$

where H_∞ controller can be obtained as in Eq.(30).

where H_∞ controller can be obtained as in Eq.(30).

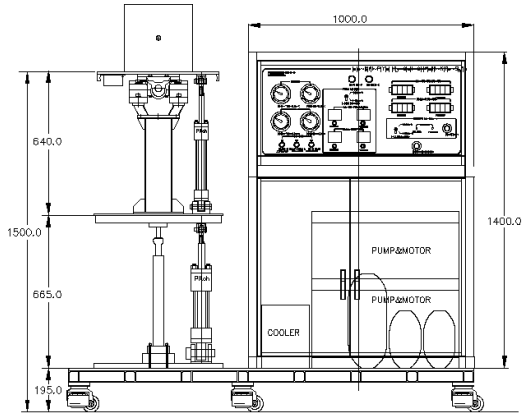

Fig. 6. Schematic diagram of gimbal system.

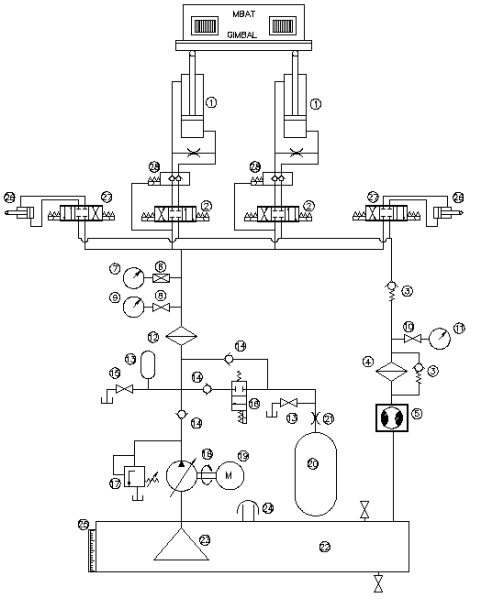

Fig. 7. Schematic diagram of electro-hydraulic.

4. Experimental equipment

The experimental equipment is divided into four parts: the hydraulic pressure providing part which produces and provides hydraulic pressure; the stability part which keeps the vessel on the horizon against the movement of the vessel; the excitation part which simulates the movement of the vessel; and the control part which applies control theories and transmit the control commands. The hydraulic pressure providing part runs a hydraulic pump by a source of electric power (220 VAC, 60 Hz, 3 phase). It is designed to adjust the flow provided to the hydraulic cylinder by servo valves (NG6,BOSCH). The stability part is designed to make it possible to individually operate and control the movement in the direction of roll and pitch by universal joint. A tiltmeter is set to measure a range of ±30°(±5 VDC) changes of the horizontal angle of each plate. For the control part, two Data Acquisition Board(DR1010) is set up in a computer (Pentium Ⅱ) and the control program is written in using LabWindows based C language. Figure 6 is the picture of the gimbal system and Fig. 7 is the schematic diagram of electro-hydraulic system which is used in this research. The nominal values of the hydraulic system parameters are listed in Table 1.

5. Results and discussion

This paper simulates and experiments using the PI controller and the H_∞ controller. The gain of the PI controller is given as K_p=60 and K_i=0.2. These give similar response characteristics of H_∞ controller for the step input. As for the uncertainty of the system, the changes of flow gain is considered due to hydraulic pressure increase. The sine wave is added for the disturbances.

Figure 8 shows the system response where the disturbances of sine wave(0.05 Hz, ±4°) is added to the excitation part. When the PI controller is applied,

Table 1. Parameters used in the system.

Parameter	Description	Value
A_1, A_2	Effective area(head/rod)	12.5 cm^2/ 8.765 cm^2
C_{tp}	Total leakage coefficient	0.047 cm^5/kgs
K_q	Servovalve flow gain	19 $cm^3/s/cm$
P_s	Supply pressure	50 kg/cm^2
β_e	Bulk modulus	14000 kg/cm^2
τ_v	Servovalve time constant	0.01
J_o	Mass moment of inertia	5136 $kg\,cm^2$
L_s	Hydraulic cylinder stroke	19 cm

the oscillation of rolling axis is died in 3 s, However, pitching axis has continuous vibration. It is considered that this may occur because the upper plate and hydraulic piston are not connected precisely. Nevertheless, this oscillation is very weak when the controller is used. It can also be seen that the oscillation of the system does not occur in 1 s.

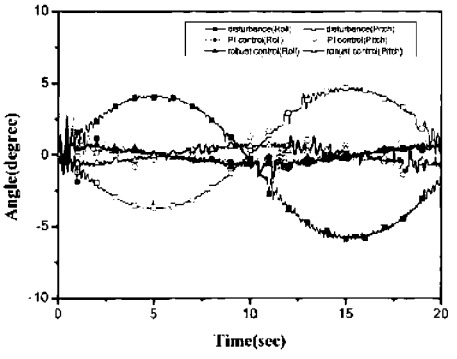

Fig. 8. Response on sine wave disturbance (0.05 Hz, ±4°).

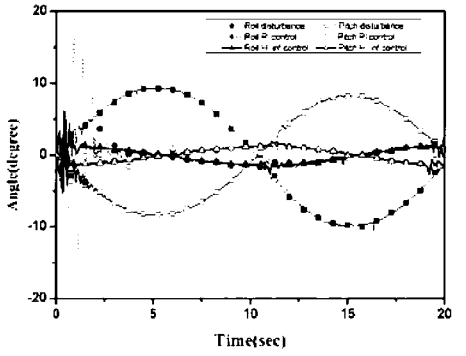

Fig. 9. Response on sine wave disturbance (0.05 Hz, ±8°).

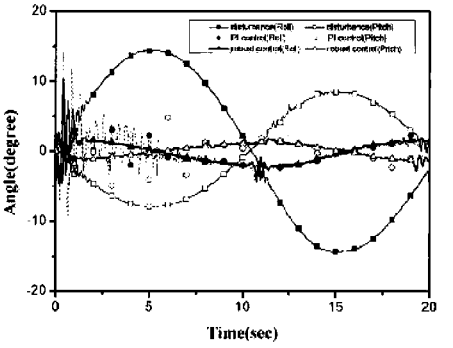

Fig. 10. Response on sine wave disturbance (0.05 Hz, ±14°, ±8°).

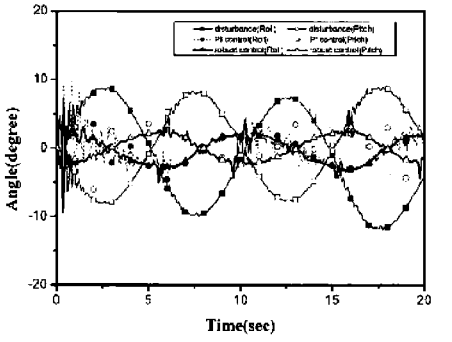

Fig. 11. Response on sine wave disturbance (0.1 Hz, ±8°).

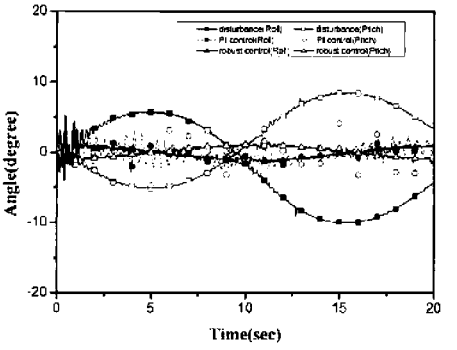

Fig. 12. Response on sine wave disturbance (0.05 Hz, +6°).

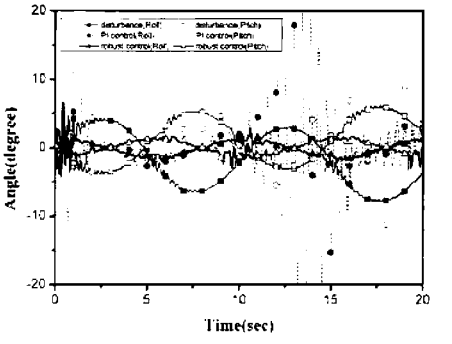

Fig. 13. Response on sine wave disturbance (0.1 Hz, ±4°).

Figure 9 shows the system response when sine wave(0.05 Hz, ±8°) is to the excitation part. For the PI controller applied, the amplitude of the initial oscillation is large, and it takes 4 s to be decayed. On the other hand, when the H_∞ controller is used, the oscillation is controlled in 1 s. Therefore, it can be seen that the initial amplitude increases regardless of the size of excitation, but the time for system's stability rapidly decreases for the robust control scheme. Figure 10 shows the system response when sine wave(0.05 Hz, ±14°, ±8°) and (0.05 Hz, ±8°) as disturbances are added to rolling axis and to pitching axis, respectively. When the PI controller is used, it can be seen that the larger amplitude the disturbance is, the longer control time the initial vibration consists. In case of the H_∞ controller, however, the initial amplitude increases regardless of the excitation intensity, but the oscillation decaying time can be quickly stabilized. Figure 11 shows the system response when sine wave(0.1 Hz, ±8°) is applied to rolling axis and pitching axis. When the PI controller is used, the amplitude of initial fluctuation becomes larger, and the control time becomes longer than that of 0.05 Hz disturbance. In addition, because the connection of the system is not precise, the vibration of system often occurs. Unlike the PI controller, when the H_∞ controller is in use, it has longer vibration control time than that of 0.05 Hz disturbance, but it shows very good stability, compared to the PI controller. Figures 12 and 13 shows how the flow and the change of pressure affect the system response where the temperature increase of hydraulic oil due to the hydraulic pump operating for many hours. When the PI controller is used, system vibration often occurs because of the change of the system. For the 0.1 Hz oscillation, the system is not stable. However, when the H_∞ controller is applied, it shows a good stability in spite of the change of the system.

6. Conclusions

In this study, through the experiment of the gimbal system which has mathematical modeling error of the system, and the model uncertainty by disturbances and sensor noise, the following conclusions obtained.

(1) The equation of motion and the mathematical modeling of a single-rod hydraulic system is derived.

(2) In order to simulate the disturbances by movement of the vessel, sine wave (0.05 Hz~0.1 Hz, ±4°~±14°) has been applied, and the PI controller and the H_∞ controller have been applied.

(3) For the PI controller with the system uncertainties, the settling time is slower and large oscillation(2°~4°) occurs during the transient period. When H_∞ controller is used, however, the settling time is 1.5 s and oscillation with 1°~2° amplitude occurs, which means that the influence by the system changes is not considerable for the H_∞ control scheme.

(4) In the case of a system which has disturbances and model uncertainty, it can be seen that the stabilization of a system can be more fully attained by the H_∞ controller than by the PI controller.

Nomenclature

A_{me}	:	Average piston area
a	:	Cross section area
B_i	:	Rotation transformation matrix
C_{tp}	:	Total leakage coefficient of the piston
$I(s)$	:	Servo valve current
K_{sv}	:	Gain of the spool displacement
L_s	:	Cylinder travel
PL	:	Load pressure
Q_D	:	Disturbance
R	:	Complementary sensitivity function
S	:	Sensitivity function
T_D	:	Load torque
V_e	:	Equivalent volume of hydraulic cylinder
X_p	:	Displacement of piston
$X_v(s)$	:	Spool displacement of servo valves
γ	:	Actuator area ratio
η	:	Flow ratio

References

Doyle, J. C., Glover, K., Khargonekar, P. P. and Francis, B. A., 1989, "State-space Solutions to Stand H_2 and H∞ Control Problems," *IEEE Trans. on Automat. Contr.*, Vol. AC-34, pp. 831~847.

Duncan McFarlane and Keith Glover, 1992, "A Loop Shaping Design Procedure Using H_∞ Synthesis," *IEEE Trans. on Automatic Control*, Vol. 37, No. 6, pp. 759~769.

Franchek, M. A., 1996 "Selecting the Performance Weights for the μ and H_∞ Synthesis Methods for SISO Regulating Systems," *Trans. of the ASME*, Vol. 118, pp. 126~131.

Lu, H. C. and Lin, W. C., 1993 "Robust Con-troller with Disturbance Rejection for Hydraulic Servo Systems," *IEEE Trans. on Industrial Electronics*, Vol. 40, No. 1, pp. 157~162.

Park, C. H., Hong, S. I. and Park, H. C., 2005, "Analytical Development of a Robust Controller for Smart Structure Systems," *KSME International Journal*, Vol. 19, No. 5, pp. 1138~1147.

Petter Lundstrom, Sigurd Skogestad and Z. Q. Wang, 1991, "Performance Weight Selection for the H_∞ and μ-control Methods," *Trans. Inst. MC*, Vol. 13, No. 5, pp. 241~252.

Postlethwaite, I., Lin, J. L. and Gu, D.W., 1991 "A Loop-shaping Approach to Robust Performance for SISO Systems," *Trans. Inst. MC*, Vol. 13, No. 5, pp. 262~268.

Watton, J., 1984, "The Generalized Response of Servovalve-controlled, Single-rod, Linear Actuators and the Influence of Transmission Line Dynamics," *Journal of Dynamic Systems,* Measurement, and Control, Vol. 106, pp. 157~162.

Yoo, Sam-Hyeon and Lee, C. W., 2001 "Robust Control of the Nonlinear Hydraulic Servo System Using a PID Control Technique," *Journal of the Korea Society of Mechanical Engineers*, Vol. 25, No. 5, pp.850~856.

Park, Y. P., Yang, H. S. and Kim, K. Y.,1996, "Active Control of Isolation Table using Control," Journal of the Korea Society of Mechanical Engineers, vol. 20, No. 10, pp. 3079～3094.

Zames, G., 1981, "Feedback and Optimal Sensitivity: Model Reference Transformation, Multiplicative Seminorms and Approximate in Verses," *IEEE Trans. Automat. Contr.*, Vol. AC-26, April, pp. 301~320.